1

Development of Texture and Substructure Inhomogeneity by Recrystallization of Rolled Zr-Based Alloys

Yuriy Perlovich and Margarita Isaenkova
National Research Nuclear University "MEPhI"
Russia

1. Introduction

Recrystallization of α-Zr is of the great interest both as a rather complicated scientific phenomenon and as a process of the practical importance for applications in the nuclear industry. Meanwhile in the most known monographs on Zr and Zr-based commercial alloys (Douglass, 1971; Tenckhoff, 1988; Zaymovskiy et al., 1994) the recrystallization of α-Zr is considered on the basis of experimental data, obtained more, than 40 years ago. These data urgently require corrections with taking into account the up-to-day theoretical conceptions and the continuous progress in experimental technique. Zr-based alloys are characterized by α↔β phase transformations within the technologically important temperature interval 610°-850°C and by operation of various mechanisms of α-Zr plastic deformation, including slip by basal, prismatic and pyramidal planes as well as twinning in several systems. These features are responsible for very complicated distribution of strain hardening and the corresponding tendency to recrystallization in products from Zr-based alloys. The given chapter makes up some gaps in our knowledge concerning different aspects of recrystallization as applied to α-Zr.

2. Regularities of recrystallization in sheets and tubes of Zr-based alloys with multicomponent rolling textures

The most widespread data on recrystallization regularities in α-Zr pertain to sheets and tubes with the final stable rolling texture of α-Zr (0001)±20°-40° ND-TD <10$\bar{1}$0> (Douglass, 1971), where ND – normal direction and TD – transverse direction. Meanwhile later the new detailed data were obtained concerning texture development in α-Zr under rolling. In particular, it was established that by rolling of a textureless slab the intermediate texture (0001) ±15°-25° ND-RD <11$\bar{2}$L> forms, where RD – rolling direction, and keeps its stability up to the deformation degree of 70%, whereupon it converts to the final stable texture (Isaenkova & Perlovich, 1987a, 1987b). Main components of these textures in the order of formation were denoted as T1 and T2. Besides, components (0001)<10$\bar{1}$0> (T0) and {11$\bar{2}$0}<10$\bar{1}$0> (T3) are present often in textures of rolled sheets and, especially, tubes. All these texture components form owing to activity of concrete combinations of plastic deformation mechanisms, have their characteristic strain hardening and therefore show

different tendencies to recrystallization. In the real case of a multicomponent texture the development of recrystallization must be additionally complicated by interaction between different components in regions of their contact. Indeed, according to (Isaenkova et al., 1988; Perlovich et al., 1989), resulting changes of α-Zr rolling textures in the course of recrystallization can not be reduced to 30°-rotation around basal normals and require for more complex description. In order to investigate this question in more details, the following work was undertaken.

2.1 Materials and methods

Recrystallization was investigated in sheet samples of alloys Zr-2,5%Nb, Zr-2,3%Cr and pure Zr as well as in tube samples of the alloy Zr-2,5%Nb. Sheets were produced by longitudinal or transverse cold rolling up to deformation degrees in the range from 40% to 90% in such a way as to form the following textures: T1, T1+T2, T2, T1+T2+T3. The weak component T0 was present everywhere. Perfection parameters and mutual relationship of different components varied. The channel tube was cold-rolled by 50%-thinning of its wall. All samples were annealed in dynamic vacuum at temperatures 500°-600°C during 1-5 h.

The main used method was X-ray diffractometric texture analysis. Direct pole figures (PF) (0001), $\{11\bar{2}0\}$ and $\{10\bar{1}2\}$ were measured by the standard procedure (Borodkina & Spector, 1981). To reveal PF regions, where texture changes by recrystallization are predominantly localized, diagrams of PFs subtraction (SD) were calculated and constructed. SD involves contours of pole density equal changes, having been drawn by comparison of recrystallization and rolling textures. In addition, PF sections of interest were constructed to follow redistribution of basal and prismatic normals in the course of recrystallization.

2.2 Recrystallization in sheets

Analysis of PFs $\{11\bar{2}0\}$ shows that texture changes by recrystallization can be described as rotation around the motionless basal axis only in the case of the rolling texture consisting largely of the component T2. However, the angle of such rotation varies: e.g. in the case of cold rolling by 60% for pure Zr recrystallized at 500°C this angle is equal to 30°, while for the alloy Zr-2,5%Nb recrystallized at 580°C – only 20°. When the rolling texture consists predominantly of the component T1, recrystallization does not involve lattice rotation around basal normals, - this is confirmed by invariance of PF$\{10\bar{1}2\}$.

Main results concern reorientation of basal normals by α-Zr recrystallization, i.e. changes of PF(0001). Superposition of SD and PF(0001) is shown in Fig. 1 for the sheet alloy Zr-2,5%Nb rolled up to deformation degrees 40, 60 and 80%, corresponding to formation of different textures: T1, T1+T2, T2. The densest cross-hatching indicates zones, where texture are localized predominantly. These zones are situated at slopes of initial texture maxima, increasing scattering of the recrystallization texture. Hence, the model of inhomogeneous strain hardening, proposed in (Perlovich, 1994) for textured BCC-metals, is true for HCP α-phase also. But while taking into account the multicomponent character of observed rolling textures, regularities of recrystallization should be more complicated.

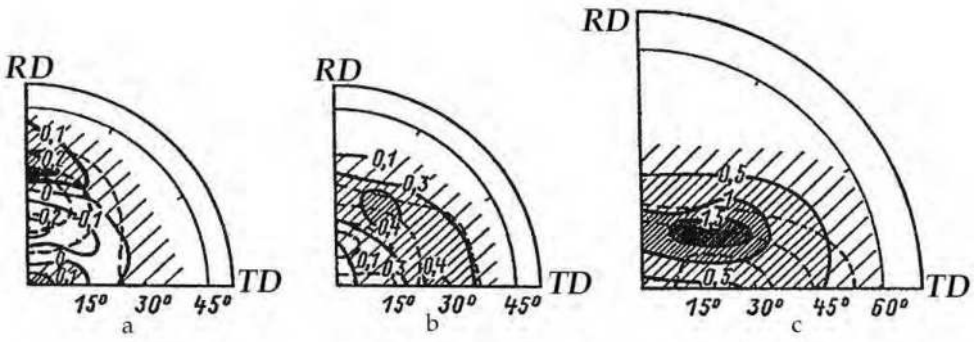

Fig. 1. Superposition of partial PF(0001) (dotted contours) for rolled sheets of the alloy Zr-2,5%Nb by deformation degrees 40% (a), 60% (b), 80% (c) and SD (solid contours), characterizing texture changes by recrystallization. Cross-hatching density reflects an increase of pole density by recrystallization.

For rolling textures T1+T2, where I(T1)>I(T2), it was established that the relative increase of main different components in the recrystallization texture depends on the initial relationship of these components in the rolling texture. In particular:

$$\Delta I(T2)/\Delta I(T1)=f_1[I(T2)/I(T1)], \quad (1)$$

$$\Delta I(T2)/\Delta I(T0)=f_2[I(T2)/I(T0)]. \quad (2)$$

These dependences are drawn in Fig. 2, where linearity of f_1 and nonlinearity of f_2 are evident. The nearer are initial intensities of components T2 and T1, the greater is difference between growth rates of new grains with corresponding orientations. As an area of the

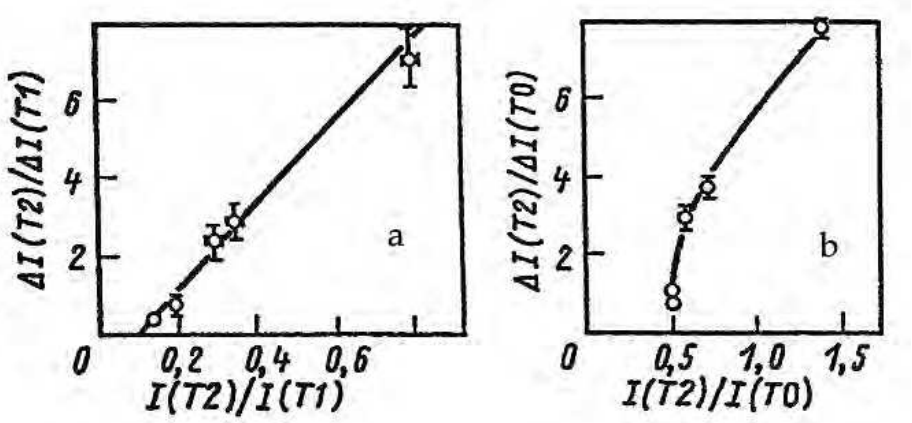

Fig. 2. Relative changing of texture components T2 versus T1 (a) and T2 versus T0 (b) in the recrystallization texture of sheet samples depending on the initial relationship of these components in the rolling texture.

contact surface between deformed grains of these components increases, conditions for growth of grains with the orientation T2 become more favorable. This signifies that T2-grains are growing into T1-grains and absorb them. The weaker dependence connects growths of components T2 and T0 in the recrystallization texture, since the difference between their strain hardening is less than in the case of components T2 and T1. Recrystallization of samples, showing predominance of the component T1, involves essential redistribution of basal normals even to the point of main texture component changing; then, depending on the concrete relationship of components in the rolling texture, T1 can give way to T0 (Fig. 3-a) or T2 (Fig. 3-b). Composition of the alloy influences mainly temperature parameters of the recrystallization process in α-Zr and seems to be of secondary importance for orientation regularities.

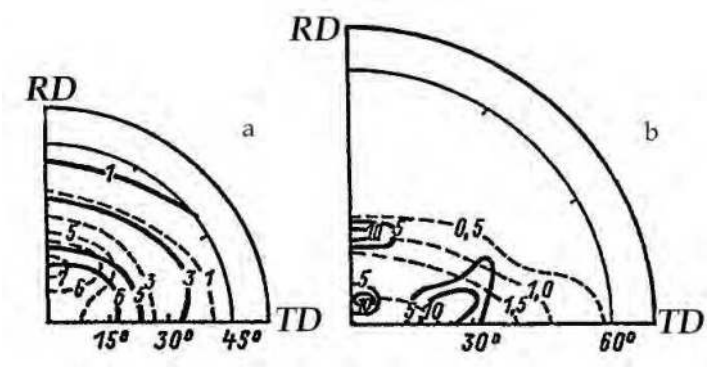

Fig. 3. Partial PF (0001) for sheet alloys Zr-2,5%Nb (a) and Zr-2,3%Cr (b) in rolled (dotted contours) and recrystallized (solid contours) states.

2.3 Recrystallization in tubes

The rolling texture of investigated tubes exhibits predominance of the component $\{11\bar{2}0\}<10\bar{1}0>$ and contains the intensive axial component with the axis $<10\bar{1}0>$ (Fig. 4). Distributions of X-ray reflection (0004) registered intensity in the PF section R-T (radial direction – tangential direction) both for rolled and annealed samples are presented in Fig. 5-a. Redistribution of registered intensity in consequence of tube annealing at 500°C is connected with a general increase of the intensity level by recovery (compare curves 1 and 2 in Fig. 5) and testifies about inhomogeneous recovery in grains with different orientations, resulting from their previous inhomogeneous strain hardening. The most active recovery is localized in grains with basal normals deflected from R-direction by 50°-60° and 90°. Hence, grains with such orientations have the greatest strain hardening and should show the maximal tendency to recrystallization. The curve 2 characterizes the true texture of the rolled tube better, than the curve 1, whose appearance on the inhomogeneous distribution of lattice defects in grains with different orientations.

As the annealing temperature increases, recrystallization process becomes more active and a sharp decrease of pole density near T-direction occurs, testifying about reorientation of basal normals. This effect is especially strong by passing from curve 4 to curve 5 (Fig. 5-a). An increase of the annealing temperature results in shifting of the maximum in the distribution of

basal normals to R-direction: after annealing at 550°C is at angular distance of 45° from R-direction, while after annealing at 600°C – at a distance of 60°. The maximum corresponds to grains, which by recrystallization are in favorable conditions for growing, though their initial strain hardening is not maximal. These grains respond to the compromise variant: their strain hardening is so high, that the accumulated energy of lattice distortion ensures their sufficiently quick growth under recrystallization annealing, and at the same time the volume fraction of these grains is sufficiently large for absorption of a significant part of the deformed matrix.

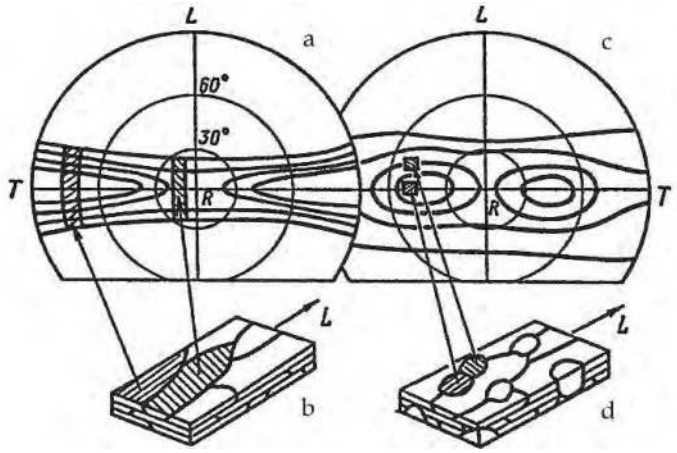

Fig. 4. PF(0001) (a, c) schematic images of microstructure (b, d) for the tube of the alloy Zr-2,5%Nb in rolled (a, b) and annealed (c, d) states. The microstructure (d) corresponds to the initial stage of recrystallization.

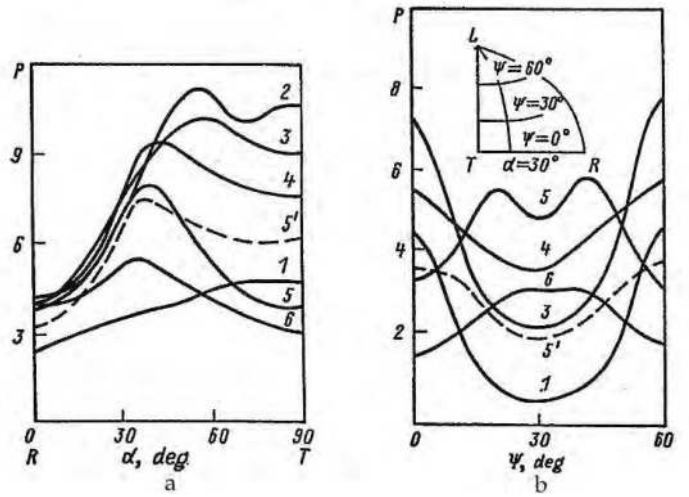

Fig. 5. Intensity distribution in the section R-T of PF(0001) (a) and in the section R-L of PF{11$\bar{2}$0} (b) for tubes of the alloy Zr-2,5%Nb: 1 – initial rolled state; 2-6 – annealing regimes: 2 - 500°C, 3 h; 3 - 530°C, 3 h; 4 - 550°C, 3 h; 5 - 580°C, 3 h; 5′ - 580°C, 1 h; 6 - 600°C, 3h.

As a result of tube annealing the new maxima arise on the meridional section of PF{11$\bar{2}$0} (Fig. 5-b), testifying that, along with redistribution of basal normals in investigated tubes, reorientation of prismatic normals takes place also, leading to development of the typical for α-Zr recrystallization texture (0001) ± α R-T <21$\bar{3}$0 – 11$\bar{2}$0 >. The situation of new maxima in the distribution of prismatic normals corresponds to slopes of initial maxima in the rolling texture, where strain hardening achieves increased values (Perlovich, 1994). The angle of misorientation between deformed and recrystallized grains by the common basal axis depends on the annealing temperature and increases from 20° to 30° when passing from annealing at 580°C to annealing at 600°C (compare curves 5 and 6 in Fig. 5-b). According to the data, presented in Fig. 5-a and 5-b, reorientation of basal normals is somewhat ahead of reorientation of prismatic normals both by time and temperature.

In order to explain the observed development of recrystallization in tubes, the model was proposed, suggesting operation of two different recrystallization mechanisms: (1) growth of new grains with intermediate orientations at high-angle boundaries between regions, having different local textures and originating from different initial grains; (2) growth of new grains with orientations, corresponding to zones of increased strain hardening within rolled initial grains. After rolling up to high deformation degrees, a polycrystal consists of thin plate-like grains, which have their own local textures and contain only low-angle subboundaries. Such structure is shown in Fig. 4-b. Then the first mechanism causes formation of new grains with intermediate orientations of basal normals, as it is shown in Fig. 4-c,d, while the second mechanism results in lattice rotation about basal normals owing to gradual growing of nuclei in zones of increased strain hardening within plate-like grains. Absorption of the deformed matrix by nuclei of new grains, growing along T- and R-directions, is controlled by structure anisotropy of a rolled tube.

Thus, it was shown that by recrystallization of α-Zr along with previously described lattice rotation around basal normals a significant redistribution of these normals takes place both in sheets and tubes. Contrary to the widespread idea, the recrystallization texture of α-Zr varies in a wide range depending on the relationship of main components in the rolling texture.

3. Substructure inhomogeneity of recrystallized sheets from Zr-based alloys

The substructure inhomogeneity is a generally recognized feature of deformed metal materials, controlling the process of their recrystallization. Since the plastic deformation usually is accompanied by arising of the crystallographic texture, developments of the substructure inhomogeneity and the deformation texture prove to be mutually interconnected. It was shown by means of X-ray diffractometric methods (Perlovich et al., 1997; 2000; Perlovich & Isaenkova, 2002), that an actual spectrum of substructure conditions in rolled metals and alloys is extremely wide and that the optimal criterion for systematization of observed substructure inhomogeneities is the grain orientation. The main principle of substructure inhomogeneity is the following: by passing from texture maxima to texture minima, grains (subgrains, blocks etc.) become finer and the lattice distortion increases. A question arises whether the recrystallization removes this inhomogeneity or recrystallized material partially retains it, contrary to the widespread viewpoint concerning its negligible scale.

The above question is very actual as applied to commercial Zr-based alloys in connection with their usage as responsible construction materials in nuclear reactors. The final heat treatment of products of Zr alloys is aimed to attain the stability of their structure and to remove residual stresses of all kinds. The recrystallization is usually believed to satisfy these requirements, since experimental evidences of its efficiency are restricted by those, accessible by standard methods of structure characterization. But standard X-ray methods are selective, i.e. obtained data relate only to grains with some definite orientation, corresponding to their reflecting position by the used measurement geometry. Therefore, these data can be considered as sufficient only under a supposition that recrystallization practically removes the substructure inhomogeneity of products. An aim of the given study is to demonstrate the real substructure inhomogeneity of recrystallized products of Zr-1%Nb and Zr-2.5%Nb alloys using special methods of modern X-ray diffractometry.

3.1 The X-ray method of generalized pole figures

Recent development of X-ray diffractometric technique allowed to elaborate a new method of the fullest description of textured metal materials with taking into account their substructure inhomogeneity. The method involves repeated recording of X-ray line profiles by the geometry of texture measurements, so that, as opposed to the standard description of the substructure by parameters of the X-ray reflection (hkl) from crystallographic planes {hkl} of the single orientation, now the substructure condition of the sample can be characterized by the multitude of line profiles, corresponding to planes {hkl} within grains of different orientations.

The treatment of measured data includes correction for the defocalization effect, approximation of X-ray line profiles with pseudo-Voight functions, calculation of their integral intensity I, physical half-width β and peak position 2θ, construction of distributions $I(\psi,\varphi)$, $\beta(\psi,\varphi)$, $2\theta(\psi,\varphi)$ in the stereographic projection of the sample, where (ψ,φ) – coordinates of reflecting planes {hkl}. These distributions, named Generalized Pole Figures (GPF), characterize substructure conditions along axes <hkl> by all their space orientations. In particular, normalized GPF $I_{hkl}(\psi,\varphi)$ is the usual texture pole figure PF{hkl}, GPF $\beta_{hkl}(\psi,\varphi)$ exhibits the combined effect of coherent block size D_{hkl} and lattice distortion $\Delta d/d_{hkl}$, GPF $2\theta(\psi,\varphi)$ describes the anisotropic elastic deformation $\varepsilon_{hkl}(\psi,\varphi)$ of grains along axes <hkl> due to action of residual microstresses.

The measured GPF $2\theta_{hkl}(\psi,\varphi)$ can be recalculated into GPF $d_{hkl}(\psi,\varphi)$ and further – into GPF $\varepsilon_{hkl}(\psi,\varphi)$, where $\varepsilon_{hkl}(\psi,\varphi) = [d(\psi,\varphi)-d_{av}]/d_{av}$ and d_{av} – the averaged weighted value of interplanar spacing d_{hkl}. Depending on the sign of ε_{hkl}, elastic extension or elastic contraction takes place along axis <hkl> with coordinates (ψ,φ), so that GPF $\varepsilon_{hkl}(\psi,\varphi)$ allows to reconstruct a deformation tensor for grains of main texture components.

Diagrams of the correlation between different GPF are very useful by the analysis of regularities, controlling formation of the inhomogeneous substructure in real metal materials by their technological treatment. These diagrams are constructed in coordinates (β_{hkl}, I_{hkl}) or $(2\theta_{hkl}, I_{hkl})$, so that each their point corresponds to some point (ψ_i,φ_j) in the stereographic projection of the sample and in GPF of reference. When taking into account, that each crystallite of α-Zr, having HCP lattice, has only one axis <0001>, volume fractions of grains with different physical broadening β and peak positions 2θ of X-ray reflections

from basal planes (0001), as well as with different values of derivative substructure characteristics along c-axis, can be determined. With this aim for all points (ψ,φ) of PF (0001) values of pole density are recalculated into weight coefficients to be used by the statistical treatment of GPF for the parameter of interest.

3.2 Experimental details and results

Substructure features of recrystallized plates of Zr-1%Nb and Zr-2.5%Nb alloys were studied. Plates were obtained by plain and transverse cold rolling by $\varepsilon \cong 55\%$ of bars, which were cut out from the annealed slab 2 mm in thickness. The direction of cold rolling coincided either with RD of the initial slab or with its TD. All plates were annealed in the evacuated vessel at 580°C during 3h, so that in both alloys the recrystallization of the dominant α-Zr phase took place. The full cycle of X-ray measurements as applied to all plates was carried out twice, that is after rolling and after annealing. The X-ray study was preceded by etching of samples, aimed to remove the surface layer ~40 μm in thickness.

By X-ray studies the texture diffractometer SIEMENS D500/TX with a position sensitive detector was used. The profile of the same X-ray line was registered by each of 1009 successive positions of the sample in the course of texture measurement. For the data treatment both the supplied software and the original programs, elaborated by authors, were applied. All data, obtained for recrystallized samples, are considered in comparison with data for the same samples in the rolled state.

In Fig. 6 incomplete GPF are presented for studied samples both in rolled and recrystallized conditions. All GPF were constructed by measurements of the X-ray line $(0004)_{\alpha\text{-}Zr}$. In Fig. 7 distributions of volume fractions of grains, characterized by different half-widths β of the X-ray line (0004) and by different values of interplanar spacing d_{0001} are constructed for some studied samples. Fig. 8 shows correlation diagrams of GPF $\beta_{0004}(\psi,\varphi)$ and GPF $2\theta_{0004}(\psi,\varphi)$ with PF(0001) for as-rolled (o) and annealed (+) samples.

3.3 Features of obtained distributions

Consideration of obtained data allows to establish the following:

1. As a result of recrystallization, the texture of α-Zr in studied plates changes in accordance with principles, revealed in section 1, so that mutual ratios of main components in the recrystallization texture depend on these ratios in the rolling texture. The most sharp texture changes accompany recrystallization in the Zr-1%Nb plate, obtained by transverse rolling (Fig. 6): the texture with predominance of components (0001)±15°÷20°ND-RD <10.L>, stable by intermediate deformation degrees, transforms into the texture of the central type.
2. Though the significant part of α-Zr crystallites by recrystallization shows a drop of the physical broadening of X-ray line (0004) down to minimal measurable values (Fig. 7), corresponding to the coherent domain size above ~150 nm, the substructure inhomogeneity of all annealed samples is still rather essential and its general character remains the same, i.e. coherent domains becomes smaller and lattice distortions increases by passing from central regions of texture maxima to their periphery. In GPF β(ψ,φ) regions with the most perfect substructure are darkened, so that its perfection increases with the degree of darkening (Fig. 6).

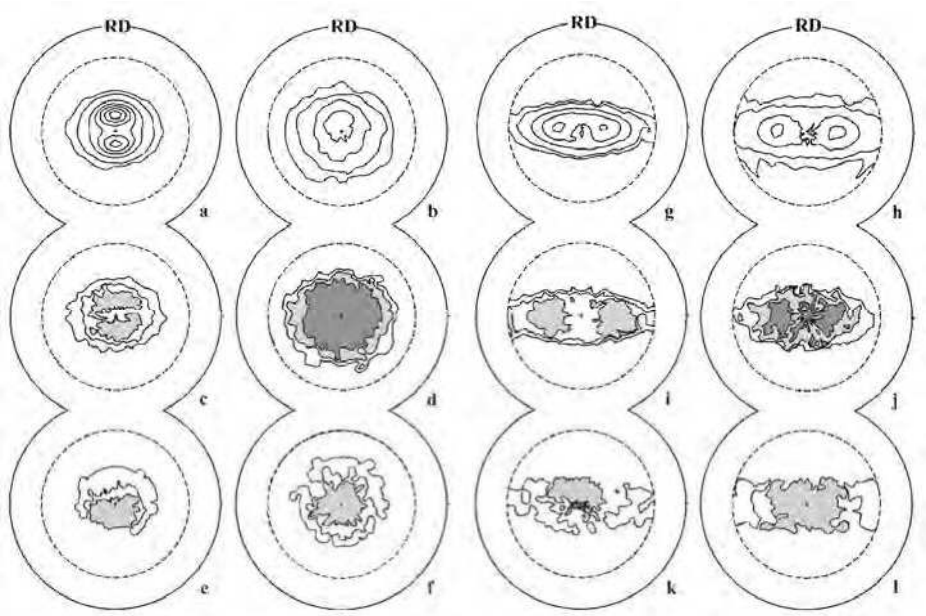

Fig. 6. PF(0001) (a, b, g, h), GPF β_{0004} (c, d, i, j) and GPF ε_c (e, f, k, l) for α-Zr: Zr-1%Nb, transversal rolling, deformed state - (a, c, e), annealed state - (b, d, f); Zr-2.5%Nb, plain rolling, deformed state - (g, i, k), annealed state - (h, g, l). Darkening: GPF β - the dark weakens from β_1= 0,2° to β_2= 0,8°; GPF ε_c – the dark shows regions with ε_c< 0.

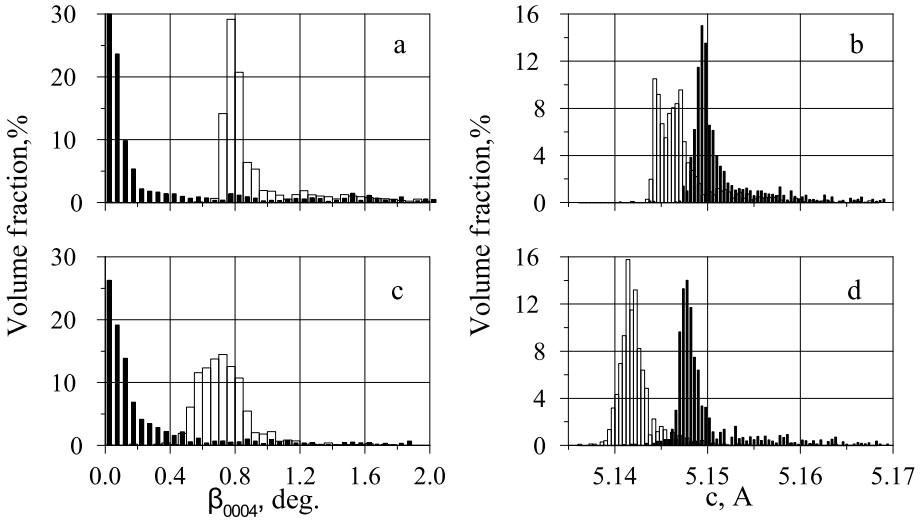

Fig. 7. Volume fractions of α-Zr crystallites with different values of X-ray line broadening β_{0004} (a, c) and lattice parameter "c" (b, d): Zr-1%Nb, transversal rolling – (a, b); Zr-2.5%Nb, plain rolling – (c, d). White columns – deformed state, black columns – annealed state.

3. Contours of equal line broadening in GPF $\beta(\psi,\varphi)$ for recrystallized plates follow contours of equal pole density in their PF(0001), testifying that the substructure inhomogeneity of annealed samples depends on the recrystallization texture and is not connected with their initial rolling texture. Hence, recrystallized plates do not succeed their substructure inhomogeneity to deformed material, but development of this inhomogeneity accompanies formation of the recrystallization texture.
4. Recrystallization results in the decrease of the average elastic microstrain, but nevertheless there are regions in GPF $\varepsilon_{0001}(\psi,\varphi)$ for recrystallized samples, where $\Delta c/c_{av}$ attains rather high values, comparable with those for as-rolled samples. In the orientation space a redistribution of elastic contraction and elastic extension along basal axes takes place in the course of recrystallization (Fig. 6), resulting in the change of the mode of microstress equilibrium (Perlovich et al., 1998): crystallites of rolled α-Zr experience residual contraction and extension along axes <0001>, deflected predominantly in opposite directions from the plane ND-TD, whereas in recrystallized α-Zr the region of elastic contraction surrounds ND and regions of elastic extension are shifted to the plane TD-RD.
5. The increase of c-parameter by recrystallization (Fig. 7) is connected with annealing of lattice defects and with leaving of excessive Nb atoms from the α-Zr solid solution in accordance with the balanced phase diagram (Douglass, 1971). Therefore, the difference in average values of c-parameter between rolled and annealed samples proves to be greater for the alloy with the higher content of Nb (2.5%).
6. In diagrams of correlation between GPF $2\theta_{0004}(\psi,\varphi)$ and PF(0001) (Fig. 8) it is distinctly seen that as a result of recrystallization the distribution of interplanar spacing d_{0001} does not become more homogeneous, than it was in the same sample after rolling; but it acquires the more regular character. Quite evident submission of interplanar spacings in recrystallized samples to usual statistical regularities reflects spontaneity of thermally activated processes, whereas in as-rolled samples these regularities are suppressed by forces, controlling plastic deformation processes.

Obtained experimental evidences of the essential substructure inhomogeneity in recrystallized Zr-based alloys depending on their texture prompt a number of inferences, connecting different aspects of recrystallization:

- The recrystallization texture includes a wide spectrum of grain orientations, so that a significant mutual misorientation of neighboring grains is probable.
- Significant microstrains can arise by meeting of neighboring growing grains and, as a result, a local elastic deformation and an increase of the dislocation density take place within boundary regions.
- Formation of specific dislocation arrangements near grain boundaries are accompanied by some local lattice rotations, so that by passing from the central part of a grain to its periphery the orientation changes, at least, by several degrees.
- Texture minima, where the fraction is localized with the most distorted crystalline lattice and finest coherent blocks, correspond to regions near boundaries of recrystallized grains.

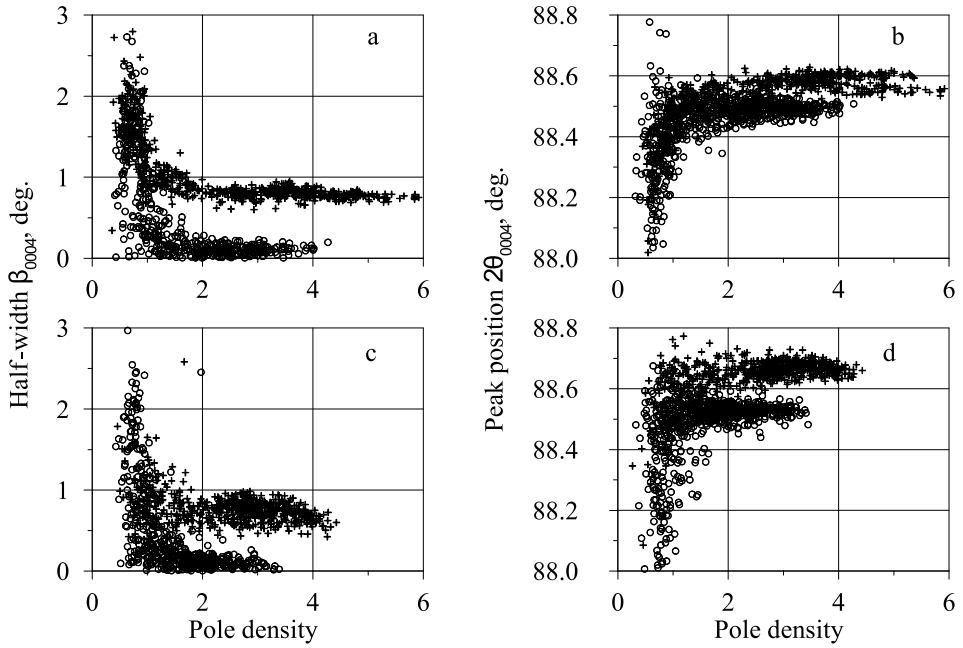

Fig. 8. Correlation diagrams for GPF β_{0004} and PF(0001) - (a, c), GPF $2\theta_{0004}$ and PF(0001) - (b, d): Zr-1%Nb, transversal rolling - (a, b); Zr-2.5%Nb, plain rolling – (c, d). Designation: + - deformed state, o - annealed state.

4. Texture of dynamic recrystallization

The question about an effect of dynamic recrystallization on the texture of rolling at increased temperatures emerges often by study of products from Zr-based alloys. This question is of the general interest and can be answered only by the rather attentive investigation of semi-products, produced at intermediate technological stages. An example of such investigation is presented below.

4.1 Materials, experimental approach and results

Sheets from Zr-2.5%Nb alloy, rolled at 750°C by two deformation routs down to thickness of ~4 mm, were studied. The used routes A and B differ in values of reduction per pass, diminishing in the order A→B, in numbers of successive passes and in presence of intermediate heating. The smaller are reductions per pass, the longer is the rolling procedure and the more significant is cooling of the billet (Perlovich et al., 2006). For compensation of this cooling the intermediate heating is introduced in route B. The alloy Zr-2.5%Nb contains usually two phases - the prevalent low-temperature HCP α-phase and the secondary high-temperature BCC β-phase. The temperature boundaries of (α+β)-region for Zr-2.5%Nb alloy are 610° and 830°C (Douglass, 1971), so that the studied sheets were rolled at the temperature of (α+β)-region, but local temperatures as well as the phase composition of concrete layers under rolling depended on their distance from the surface.

The layer-by-layer study of rolled sheets was carried out by X-ray diffractometric methods and mainly – by texture analysis. Texture analysis of α-Zr included measurement and construction of direct pole figures PF(0001) and PF{11$\bar{2}$0}. Typical PF(0001) and PF{11$\bar{2}$0} for surface, intermediate and central layers of the hot-rolled sheet are presented in Fig. 9. When passing from the surface layer of sheet to the central one, the rolling texture changes essentially. The following characteristic features of the rolling texture are considered: (1) the angular distance γ of texture maxima from normal direction (ND) in PF(0001); (2) the presence of additional texture maxima in PF{11$\bar{2}$0}, arising usually by recrystallization at the angular distance of 30° from maxima of the deformation texture. In PF{11$\bar{2}$0} (Fig. 9) these maxima are denoted by letters R and D, respectively. Layer-by-layer changes of angle γ are shown in figure 10-a; the layer-by-layer inhomogeneity of recrystallization is characterized by changes of ratio P_{recr}/P_{def} in Fig. 10-b, where P_{recr} and P_{def} – intensities of corresponding texture maxima.

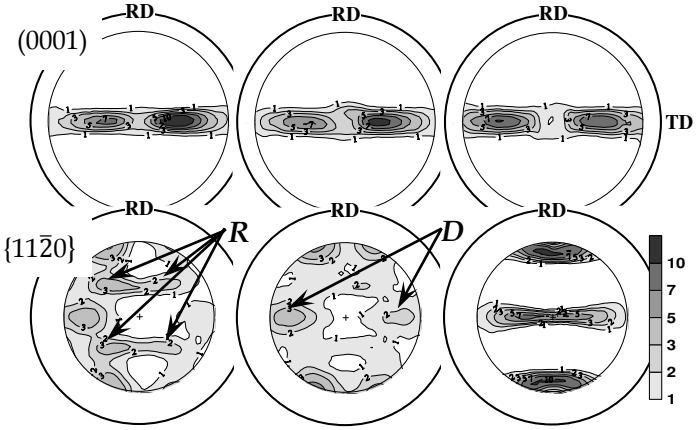

Fig. 9. Typical PF(0001) and PF{11$\bar{2}$0} for surface, intermediate and central layers of the hot-rolled sheet. Angular radius of constructed PF(0001) is equal to 80°, PF{11$\bar{2}$0} – 70°.

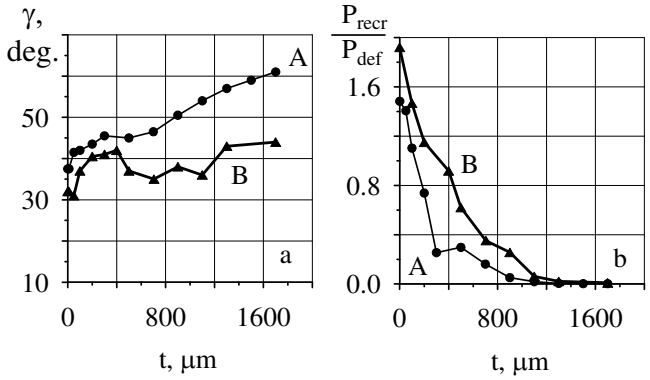

Fig. 10. Layer-by-layer changes of texture characteristics across the thickness of hot-rolled sheets: a – angular distance γ of texture maxima from ND in PF(0001); b - ratio P_{recr}/P_{def}, measured by PF{11$\bar{2}$0}.

4.2 Dynamic recrystallization under rolling

Development of recrystallization in α-Zr under rolling is seen in the surface layer up to 0.8 mm thick (Fig. 10-b). In PF{11$\bar{2}$0} of this layer (Fig. 9) maxima of rolling and recrystallization textures are present simultaneously, testifying that recrystallization of the sheet was only partial. Since texture maxima D and R are lying on different meridians, it is clear, that recrystallization included only grains with basal axes, closest to TD. Fig. 9 demonstrates visually the layer-by-layer inhomogeneity of α-Zr recrystallization in hot-rolled sheets. The angular shift of texture maxima in PF(0001) by passing from surface to central layers (Fig. 10-a) testifies in accordance with results of section 2, that recrystallization involves the reorientation of basal axes along with the known rotation of prismatic axes.

One more noteworthy difference between texture maxima D and R consists in their shape: maxima R are narrow and stretched along parallels of PF, likewise texture maxima in corresponding PF(0001), whereas maxima D are roundish and almost equiaxial. The shape of maxima R is a distinct evidence of dynamic recrystallization: anisotropic development of diffusion processes under hot rolling, including dislocation climb, results in stretching of texture maxima, as it is typical for rolling textures.

And vice versa, when the structure reforms spontaneously, only due to thermal activation, preferred directions in displacements of dislocations and dislocation boundaries are absent, so that texture maxima prove to be equiaxial, as it is usual for textures of static recrystallization. Then the round shape of maxima D in the rolling texture shows, that corresponding grains of α-Zr had time for polygonization in the course of cooling. A volume fraction of recrystallized grains decreases with distance from the surface, since stress relaxation in inner layers occurs by means of α→β→α phase transformations.

By route B the layer of dynamic recrystallization is thicker, than by route A (Fig. 10-b), because this process most probably develops in α-region of Zr-Nb phase diagram and the temperature boundary between α- and (α+β)-regions shifts deep into the sheet by passing from route A to route B in consequence of more intense cooling.

Thus, presented experimental results show, that by rolling of sheets from Zr-2.5%Nb alloy at the temperature 750°C a significant gradient in deformation conditions across the thickness of sheet takes place. The real temperature of concrete layers deviates from the nominal one due to the heat sink to rolls and local heating by deformation. A decrease of the deformation rate promotes development of dynamic recrystallization, suppresses the deformation-induced α→β phase transformation and weakens the unfavorable texture component, formed by rolling in β-phase.

5. Competition between recrystallization and phase transformations by welding of sheets from Zr-2,5%Nb alloy

The usual temperature of recrystallization annealing for α-Zr in cold-rolled products from Zr-based alloys is 580°C, that is close to the lower boundary of the (α+β)-region in the Zr-Nb phase diagram (610°C), where phase transformation (PT) α→β begins. Therefore under conditions of some heat treatments a competition is probable between recrystallization of α-Zr and PT α→β. In particular, such conditions take place by welding of cold-rolled sheets from Zr-based alloys in the thermal influence zone (TIZ) of the welding seam. When taking

into account the regular difference between textures of sheets, experienced PT α→β without and after preliminary recrystallization (Cheadle & Ells, 1966), the inhomogeneity of recrystallization within TIZ of the welding seam was analyzed.

5.1 "Multiplication" of maxima in α-Zr texture by phase transformations α→β→α

The preliminary recrystallization of α-Zr influences the texture, which arise in the sheet as a result of PT α→β→α due to realization of the Burgers orientation relationship between α- and β-phases (Douglass, 1971):

$$(0001)_\alpha \parallel \{011\}_\beta,\ <11\bar{2}0>_\alpha \parallel <111>_\beta.$$

Multiplication of initial orientations in consequence of PT α→β→α was analyzed in (Cheadle & Ells, 1966). By absence of variant selection, 35 new orientations of the basal plane arise in addition to the initial one; by mutual coincidence of some orientations their total number decreases down to 24. Since in reality we deal with textured polycrystals of Zr-alloys instead of single crystals, after PT α→β→α the resulting distribution of basal axes in PF(0001) consists of overlapping texture maxima rather than of separate points. Therefore some new orientations of 24 above-mentioned ones, being close to each other, form common maxima. Thus, PT complicates an initial texture, multiplying its maxima in a definite way, though the resulting PF(0001) of the treated sample contains a lesser number of separate maxima, than the Burgers relationship predicts.

5.2 Studied samples and investigation technique

Samples for investigation were cut from sheets of the Zr-2,5%Nb alloy, cold-rolled up to the deformation degree of ~80%. In order to prepare semi-recrystallized samples, after cold rolling they were annealed at 550°C for 1 h. In order to induce PT α→β→α, both cold-rolled and annealed samples were subjected to the heat treatment in dynamic vacuum, including heating up to 950°C for 0,25 h, holding at this temperature during 0,5 h and subsequent cooling with an evacuated envelope in air. X-ray texture measurements were carried out by the standard method (Borodkina & Spector, 1981) using the diffractometer DRON-3M and Cu K_α radiation. For construction of complete PF, three mutually perpendicular sections of sheet or tube were investigated to obtain partial PF for their following sewing together (Perlovich & Isaenkova, 2002).

The investigated welded joints were produced by argon-arc welding of cold-rolled sheets of Zr-2,5%Nb alloy, using a non-expendable tungsten electrode with a motion velocity of 60 m/h. The welding direction (WD) was perpendicular to the RD. Texture inhomogeneity near the welding seam, connected with different heating conditions at neighboring regions, was studied layer-by-layer depending on the layer distance from the centre line of the seam.

5.3 Changes in α-Zr texture of cold-rolled and annealed sheets

PF(0001) for cold-rolled sheet is shown in Fig. 11-a, PF(0001) for the same sheet after heat treatment at 950°C – in Fig. 11-b, distributions of pole density along the radius ND-TD – in Fig. 11-c. Analogous PF and distributions for the sheet, which before PT experienced annealing at 550°C, - in Fig. 12-a,b,c. Comparison of PF(0001) in Fig. 11-a and Fig. 12-a

shows, that partial recrystallization of the cold-rolled sheet causes extension of the pole density distribution to TD. Black circles in Fig. 11-b indicate ideal positions of texture maxima, arising as a result of PT α→β→α in PF(0001) of the cold-rolled sheet, whereas black circles in Fig. 12-b – calculated positions of PT-induced texture maxima in PF(0001) of the completely recrystallized sheet. In the considered real case of the semi-recrystallized sheet these black circles get only to those texture maxima, which are absent in PF(0001) of the cold-rolled sheet. This feature testifies, that some texture maxima in PF(0001) (Fig. 12-b) are produced by "multiplication" of maxima, belonging to the rolling texture, and some others – to the recrystallization texture.

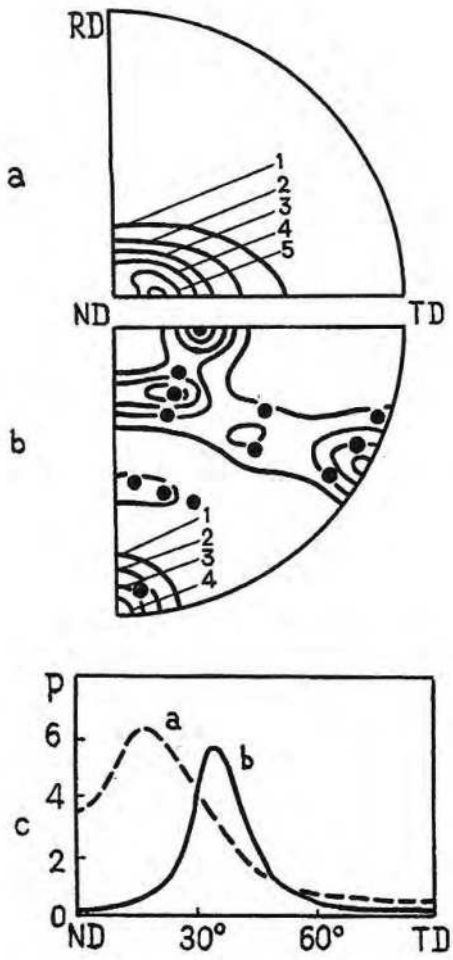

Fig. 11. PT in the cold-rolled sheet of Zr-2,5%Nb alloy, PF(0001): a – cold rolling; b – cold rolling + heat treatment 950°C/0,25 h; c – distributions of pole density along PF radius ND-TD.

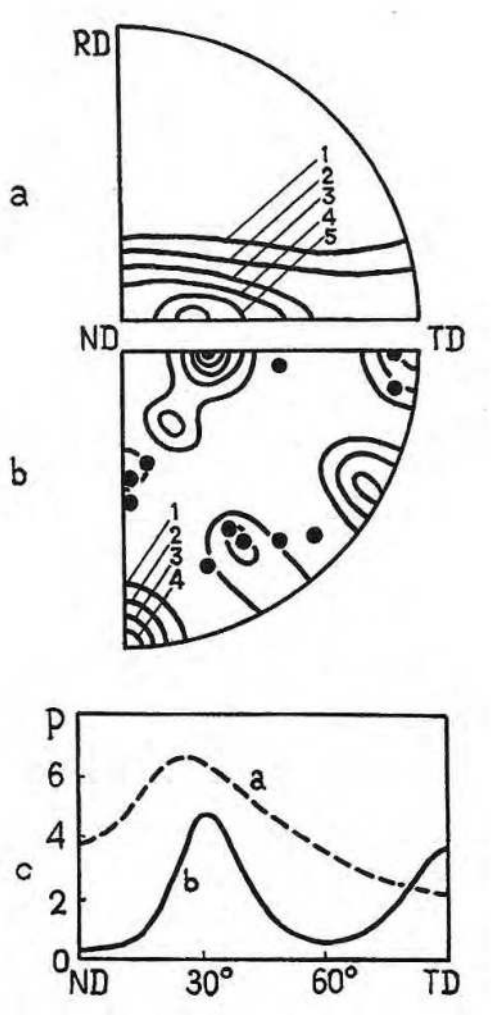

Fig. 12. PT in the semi-recrystallized sheet of Zr-2,5%Nb alloy, PF(0001): a – cold rolling + annealing 550°/1 h.; b - cold rolling + annealing 550°/1 h + heat treatment 950°/0,25 h; c - distributions of pole density along PF radius ND-TD.

In particular, as a result of PT α→β→α in recrystallized grains, a new texture component $\{10\bar{1}0\}<11\bar{2}0>$ arises, having its maximum in PF(0001) at TD. Other maxima of the same set are present at the predicted regions also, confirming additionally the fact of preliminary recrystallization in the course of heating to the β-phase. At the same time, maxima, originating from deformed α-grains, by PT become noticeably weaker, than in the case of PT without preliminary recrystallization (compare Fig. 11-b and 12-b). The real situation in the deformed textured α-phase requires a description, similar to the case of a composite; therefore it would be correct to state a possibility of different outcomes from the competition between recrystallization and PT α→β depending on deformation degree, grain orientation, heating rate, and so on. Inhomogeneous development of the considered processes, as well as their mutual competition, corresponds apparently to the most general case.

5.4 Recrystallization in the thermal influence zone by welding

Below some observations are presented concerning the competition between recrystallization and PT α→β in the thermal influence zone (TIZ) with reference to the Zr-2,5%Nb alloy.

Arc welding is accompanied by a local heat treatment of the material in the vicinity of the welding seam. Parameters of a short-time thermal cycle, passing lengthwise TIZ parallel to the welding direction, are different for each longitudinal section of TIZ and depend on its distance from the central line of the seam. Layer-by-layer study of the texture within the TIZ gives an insight into the inhomogeneous structure developed in this zone by welding. In Fig. 13-a a schematic image of a welded joint is drawn; the melting zone is denoted by dense hatching and TIZ – by thin hatching. Three longitudinal sections are shown within the TIZ, and for each section an arrow indicates the corresponding PF(0001), obtained by X-ray diffractometric study just of this section. RD is brought into the centre of these PF in contrast with above-presented PF(0001) in Fig. 11 and 12.

Judging from PF in Fig. 13, different textures have formed in the shown sections of the TIZ depending on the distance from the seam. While in the most remote section the initial distribution of basal axes remains unchanged, the textures of the two closer sections contain new components produced by PT. Pole figures for these sections differ in relationship of PT components, originated from deformed (A) and recrystallized (B) α-grains. A quantitative treatment of obtained experimental data included the calculation of parameters, characterizing the relative contributions of both deformed and recrystallized components in the measured texture. In Fig. 13-b the results of such treatment for 18 successive sections of the TIZ are presented. The upper curve, constructed by PF$\{11\bar{2}0\}$, characterizes the relative fraction of recrystallized grains depending on the distance from the seam, irrespective of whether these grains experienced PT or did not. The following curve, constructed by PF(0001), characterizes the relative fraction of recrystallized grains in volume, covered by PT; it should be noted that in the general case this volume forms only a part of the investigated layer. The lower curve was obtained by subtraction of the (0001)-curve from the $\{11\bar{2}0\}$-curve. It characterizes the fraction, falling on grains, which proved to be recrystallized, but did not experience PT.

The presented curves testify unambiguously that, by sufficient increase of the heating temperature, all grains experience recrystallization prior to PT α→β. Thus, competition

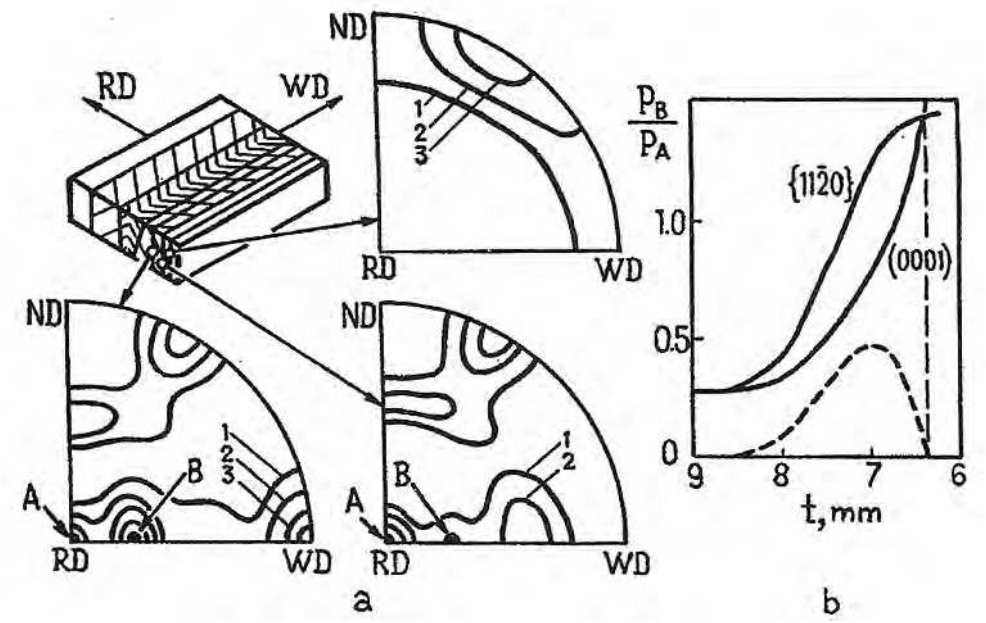

Fig. 13. PT in the thermal influence zone by arc welding: (a) the schematic image of welding seam and PF(0001) for its different section; (b) quantitative treatment of PF (see detailed explanation in the text).

between recrystallization and PT by a high rate of heating results in an absolute predominance of primary recrystallization (variant 1), though at some intermediate regimes of heat treatment two other variants are possible: recrystallization of deformed α-grains without their subsequent PT (variant 2) and PT of deformed α-grains without their preliminary recrystallization (variant 3).

Thus, the most important feature of the processes in the thermal influence zone is their inhomogeneous character, particularly by intermediate regimes of the heat treatment. While in some grains the variant 1 realizes, in other grains the variants 2 or 3 take place. The concrete variant, actual for the given grains, depends in some complicated manner on their orientation.

6. References

Borodkina M.M. & Spector E.N. (1981). *X-ray Analysis of Texture in Metals and Alloys*. Publishing House "Metallurgiya", Moscow, pp. 48-91 (in Russian).

Cheadle B.A. & Ells C.E. (1966) The effect of heat treatment on the texture of fabricated Zr-rich alloys. *Electroch. Techn*., Vol. 4, No 7-8, pp. 329-336.

Douglass D.L. (1971). *The Metallurgy of Zirconium*. International Atomic Energy Agency, Vienna, pp. 60-76.

Isaenkova M. & Perlovich Yu. (1987a). Kinetics and mechanisms of texture formation in α-Zr by rolling. *Fizika Metallov i Metallovedenie*, Vol. 64, No 1, pp. 107-112 (in Russian).

Isaenkova M. & Perlovich Yu. (1987b). Reorientation of α-Zr crystallites by deformation. *Izvestiya Akademii Nauk SSSR. Metalli*, No 3, pp. 152-155 (in Russian).

Isaenkova M., Kapliy S., Perlovich Yu. & Shmelyova T. (1988). Features of changes of the Zirconium rolling texture by recrystallization. *Atomnaya Energiya*, Vol. 65, No 1, pp. 42-45 (in Russian).

Perlovich Yu., Isaenkova M., Shmelyova T., Nikulina A. & Zavyalov A. (1989). Texture changes in tubes of the alloy Zr-2,5%Nb by recrystallization. *Atomnaya Energiya*, Vol. 67, No 5, pp. 327-331 (in Russian).

Perlovich Yu. (1994). Development of strain hardening inhomogeneity during texture formation under rolling of bcc-metals. In: *Numerical Prediction of Deformation Processes and the Behavior of Real Materials, 15th Riso International Symposium on Material Science*, 5-9 September 1994, S.I. Andersen et al. Eds, Riso National Laboratory, Roskilde, Denmark, pp. 445-450.

Perlovich Yu., Bunge H.J. & Isaenkova M. (1997). Inhomogeneous distribution of residual deformation effects in textured BCC metals. *Textures & Microstructures*, Vol. 29, pp. 241-266.

Perlovich Yu., Bunge H.J., Isaenkova M. & Fesenko V. (1998) The Distribution of Elastic Deformation in Textured Materials as Revealed by Peak Position Figures. *Material Science Forum*, Vol. 273-275, pp. 655-666.

Perlovich Yu., Bunge H.J. & Isaenkova M. (2000) Structure inhomogeneity of rolled textured niobium. *Zeitschrifft fur Metallkunde*, Materials Research and Advanced Techniques, 2000, Vol. 91, No 2, p. 149-159.

Perlovich Yu. & Isaenkova M. (2002) Distribution of c- and a-dislocations in tubes of Zr alloys. *Metallurgical and materials transactions A,* Vol. 33A, No.3, pp. 867-874.

Perlovich Yu., Isaenkova M., Akhtonov S., Filippov V., Kropachev S. & Shtutca M. (2006) Interdependence of plastic deformation and phase transformations in Zr-2.5%Nb alloy under forging by different temperature-rate regimes. *Proceedings of the 9th International Conference on Material Forming ESAFORM 2006*, Glazgow, United Kingdom, April 2006, pp. 439-442.

Tenckhoff E. (1988) Deformation mechanisms, texture and anisotropy in Zirconium and Zircaloy. - ASTM, Special technical publication (STP 966), Philadelphia, 1988. - 77 p.

Zaymovskiy A.S., Nikulina A.V. & Reshetnikov N.G. (1994). *Zirconium Alloys in Nuclear Industry.* Energoatomizdat, Moscow, ISBN 5-283-03767-3, Russia, 256 p. (in Russian).

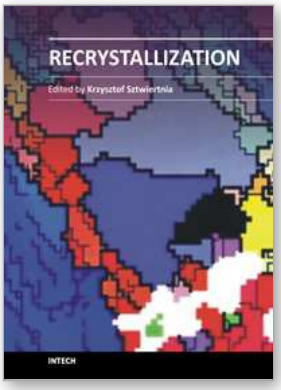

Recrystallization

Edited by Prof. Krzysztof Sztwiertnia

ISBN 978-953-51-0122-2
Hard cover, 464 pages
Publisher InTech
Published online 07, March, 2012
Published in print edition March, 2012

Recrystallization shows selected results obtained during the last few years by scientists who work on recrystallization-related issues. These scientists offer their knowledge from the perspective of a range of scientific disciplines, such as geology and metallurgy. The authors emphasize that the progress in this particular field of science is possible today thanks to the coordinated action of many research groups that work in materials science, chemistry, physics, geology, and other sciences. Thus, it is possible to perform a comprehensive analysis of the scientific problem. The analysis starts from the selection of appropriate techniques and methods of characterization. It is then combined with the development of new tools in diagnostics, and it ends with modeling of phenomena.

InTech Europe
University Campus STeP Ri
Slavka Krautzeka 83/A
51000 Rijeka, Croatia
Phone: +385 (51) 770 447
Fax: +385 (51) 686 166
www.intechopen.com

InTech China
Unit 405, Office Block, Hotel Equatorial Shanghai
No.65, Yan An Road (West), Shanghai, 200040, China
中国上海市延安西路65号上海国际贵都大饭店办公楼405单元
Phone: +86-21-62489820
Fax: +86-21-62489821